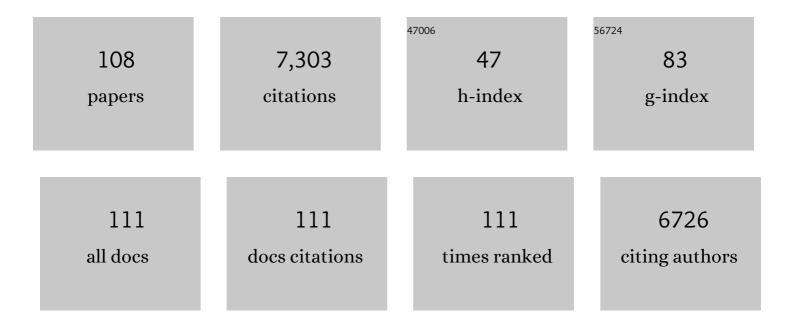
## Michael T Mcmahon

List of Publications by Year in descending order

Source: https://exaly.com/author-pdf/6662816/publications.pdf Version: 2024-02-01



#	Article	IF	CITATIONS
1	High-resolution molecular structure of a peptide in an amyloid fibril determined by magic angle spinning NMR spectroscopy. Proceedings of the National Academy of Sciences of the United States of America, 2004, 101, 711-716.	7.1	495
2	Mesoporous Silica-Coated Hollow Manganese Oxide Nanoparticles as Positive <i>T</i> <sub>1</sub> Contrast Agents for Labeling and MRI Tracking of Adipose-Derived Mesenchymal Stem Cells. Journal of the American Chemical Society, 2011, 133, 2955-2961.	13.7	491
3	Artificial reporter gene providing MRI contrast based on proton exchange. Nature Biotechnology, 2007, 25, 217-219.	17.5	379
4	Natural <scp>D</scp> â€glucose as a biodegradable MRI contrast agent for detecting cancer. Magnetic Resonance in Medicine, 2012, 68, 1764-1773.	3.0	295
5	Quantifying exchange rates in chemical exchange saturation transfer agents using the saturation time and saturation power dependencies of the magnetization transfer effect on the magnetic resonance imaging signal (QUEST and QUESP): Ph calibration for poly-L-lysine and a starburst dendrimer. Magnetic Resonance in Medicine. 2006. 55. 836-847.	3.0	288
6	Nuclear Overhauser enhancement (NOE) imaging in the human brain at 7T. NeuroImage, 2013, 77, 114-124.	4.2	266
7	Nuts and bolts of chemical exchange saturation transfer MRI. NMR in Biomedicine, 2013, 26, 810-828.	2.8	254
8	De novo determination of peptide structure with solid-state magic-angle spinning NMR spectroscopy. Proceedings of the National Academy of Sciences of the United States of America, 2002, 99, 10260-10265.	7.1	253
9	MRI-detectable pH nanosensors incorporated intoÂhydrogels for inÂvivo sensing of transplanted-cell viability. Nature Materials, 2013, 12, 268-275.	27.5	189
10	New "multicolor―polypeptide diamagnetic chemical exchange saturation transfer (DIACEST) contrast agents for MRI. Magnetic Resonance in Medicine, 2008, 60, 803-812.	3.0	188
11	MR tracking of transplanted cells with "positive contrast―using manganese oxide nanoparticles. Magnetic Resonance in Medicine, 2008, 60, 1-7.	3.0	164
12	Furin-mediated intracellular self-assembly of olsalazine nanoparticles for enhanced magnetic resonance imaging and tumour therapy. Nature Materials, 2019, 18, 1376-1383.	27.5	164
13	Dynamic Glucose-Enhanced (DGE) MRI: Translation to Human Scanning and First Results in Glioma Patients. Tomography, 2015, 1, 105-114.	1.8	153
14	Optimization of SABRE for polarization of the tuberculosis drugs pyrazinamide and isoniazid. Journal of Magnetic Resonance, 2013, 237, 73-78.	2.1	122
15	Variable delay multi-pulse train for fast chemical exchange saturation transfer and relayed-nuclear overhauser enhancement MRI. Magnetic Resonance in Medicine, 2014, 71, 1798-1812.	3.0	115
16	MRI Reporter Genes. Journal of Nuclear Medicine, 2008, 49, 1905-1908.	5.0	109
17	In vivo multicolor molecular MR imaging using diamagnetic chemical exchange saturation transfer liposomes. Magnetic Resonance in Medicine, 2012, 67, 1106-1113.	3.0	104
18	Highâ€ŧhroughput screening of chemical exchange saturation transfer MR contrast agents. Contrast Media and Molecular Imaging, 2010, 5, 162-170.	0.8	103

#	Article	IF	CITATIONS
19	An Experimental and Quantum Chemical Investigation of CO Binding to Heme Proteins and Model Systems: A Unified Model Based on13C,17O, and57Fe Nuclear Magnetic Resonance and57Fe Mössbauer and Infrared Spectroscopies. Journal of the American Chemical Society, 1998, 120, 4784-4797.	13.7	100
20	Dynamic glucose enhanced (DGE) MRI for combined imaging of blood-brain barrier break down and increased blood volume in brain cancer. Magnetic Resonance in Medicine, 2015, 74, 1556-1563.	3.0	94
21	Vaginal Delivery of Paclitaxel via Nanoparticles with Nonâ€Mucoadhesive Surfaces Suppresses Cervical Tumor Growth. Advanced Healthcare Materials, 2014, 3, 1044-1052.	7.6	85
22	Monitoring Enzyme Activity Using a Diamagnetic Chemical Exchange Saturation Transfer Magnetic Resonance Imaging Contrast Agent. Journal of the American Chemical Society, 2011, 133, 16326-16329.	13.7	83
23	In vivo high-resolution diffusion tensor imaging of the mouse brain. NeuroImage, 2013, 83, 18-26.	4.2	83
24	QUESP and QUEST revisited – fast and accurate quantitative CEST experiments. Magnetic Resonance in Medicine, 2018, 79, 1708-1721.	3.0	82
25	Rapid and quantitative chemical exchange saturation transfer (CEST) imaging with magnetic resonance fingerprinting (MRF). Magnetic Resonance in Medicine, 2018, 80, 2449-2463.	3.0	81
26	Transforming Thymidine into a Magnetic Resonance Imaging Probe for Monitoring Gene Expression. Journal of the American Chemical Society, 2013, 135, 1617-1624.	13.7	80
27	Indirect Detection of Labile Solute Proton Spectra via the Water Signal Using Frequency-Labeled Exchange (FLEX) Transfer. Journal of the American Chemical Society, 2010, 132, 1813-1815.	13.7	79
28	Advances in using MRI probes and sensors for <i>in vivo</i> cell tracking as applied to regenerative medicine. DMM Disease Models and Mechanisms, 2015, 8, 323-336.	2.4	77
29	Carbonyl Complexes of Iron(II), Ruthenium(II), and Osmium(II) 5,10,15,20-Tetraphenylporphyrinates:Â A Comparative Investigation by X-ray Crystallography, Solid-State NMR Spectroscopy, and Density Functional Theory. Journal of the American Chemical Society, 1998, 120, 11323-11334.	13.7	76
30	Salicylic Acid and Analogues as diaCEST MRI Contrast Agents with Highly Shifted Exchangeable Proton Frequencies. Angewandte Chemie - International Edition, 2013, 52, 8116-8119.	13.8	73
31	In vivo and ex vivo diffusion tensor imaging of cuprizoneâ€induced demyelination in the mouse corpus callosum. Magnetic Resonance in Medicine, 2012, 67, 750-759.	3.0	72
32	Establishing the Lysine-rich Protein CEST Reporter Gene as a CEST MR Imaging Detector for Oncolytic Virotherapy. Radiology, 2015, 275, 746-754.	7.3	70
33	Single <sup>19</sup> F Probe for Simultaneous Detection of Multiple Metal Ions Using miCEST MRI. Journal of the American Chemical Society, 2015, 137, 78-81.	13.7	70
34	Natural Dâ€glucose as a biodegradable MRI relaxation agent. Magnetic Resonance in Medicine, 2014, 72, 823-828.	3.0	69
35	Metal Ion Sensing Using Ion Chemical Exchange Saturation Transfer <sup>19</sup> F Magnetic Resonance Imaging. Journal of the American Chemical Society, 2013, 135, 12164-12167.	13.7	67
36	Experimental, Hartreeâ^'Fock, and Density Functional Theory Investigations of the Charge Density, Dipole Moment, Electrostatic Potential, and Electric Field Gradients inl-Asparagine Monohydrate. Journal of the American Chemical Society, 2000, 122, 4708-4717.	13.7	65

#	Article	IF	CITATIONS
37	Human Protamine-1 as an MRI Reporter Gene Based on Chemical Exchange. ACS Chemical Biology, 2014, 9, 134-138.	3.4	64
38	Label-free in vivo molecular imaging of underglycosylated mucin-1 expression in tumour cells. Nature Communications, 2015, 6, 6719.	12.8	62
39	Solid-State NMR, Crystallographic and Density Functional Theory Investigation of Feâ^'CO and Feâ^'CO Analogue Metalloporphyrins and Metalloproteinsâ€. Journal of the American Chemical Society, 1999, 121, 3818-3828.	13.7	61
40	Size-Induced Enhancement of Chemical Exchange Saturation Transfer (CEST) Contrast in Liposomes. Journal of the American Chemical Society, 2008, 130, 5178-5184.	13.7	61
41	Achieving 1% NMR polarization in water in less than 1min using SABRE. Journal of Magnetic Resonance, 2014, 246, 119-121.	2.1	59
42	Multimodal imaging of sustained drug release from 3-D poly(propylene fumarate) (PPF) scaffolds. Journal of Controlled Release, 2011, 156, 239-245.	9.9	58
43	MRI biosensor for protein kinase A encoded by a single synthetic gene. Magnetic Resonance in Medicine, 2012, 68, 1919-1923.	3.0	55
44	A diaCEST MRI approach for monitoring liposomal accumulation in tumors. Journal of Controlled Release, 2014, 180, 51-59.	9.9	52
45	CEST phase mapping using a length and offset varied saturation (LOVARS) scheme. Magnetic Resonance in Medicine, 2012, 68, 1074-1086.	3.0	51
46	CEST-MRI detects metabolite levels altered by breast cancer cell aggressiveness and chemotherapy response. NMR in Biomedicine, 2016, 29, 806-816.	2.8	49
47	CEST theranostics: label-free MR imaging of anticancer drugs. Oncotarget, 2016, 7, 6369-6378.	1.8	49
48	Solid-State Nuclear Magnetic Resonance Spectroscopic and Quantum Chemical Investigation of13C and17O Chemical Shift Tensors,17O Nuclear Quadrupole Coupling Tensors, and Bonding in Transition-Metal Carbonyl Complexes and Clusters. Journal of the American Chemical Society, 1998, 120, 4771-4783.	13.7	48
49	Detection of rapidly exchanging compounds using onâ€resonance frequencyâ€labeled exchange (FLEX) transfer. Magnetic Resonance in Medicine, 2012, 68, 1048-1055.	3.0	47
50	Developing imidazoles as CEST MRI pH sensors. Contrast Media and Molecular Imaging, 2016, 11, 304-312.	0.8	47
51	Liposome-based mucus-penetrating particles (MPP) for mucosal theranostics: Demonstration of diamagnetic chemical exchange saturation transfer (diaCEST) magnetic resonance imaging (MRI). Nanomedicine: Nanotechnology, Biology, and Medicine, 2015, 11, 401-405.	3.3	44
52	Tuning Phenols with Intraâ€Molecular Bond Shifted HYdrogens (IMâ€ <b>5</b> HY) as diaCEST MRI Contrast Agents. Chemistry - A European Journal, 2014, 20, 15824-15832.	3.3	43
53	Salicylic Acid Conjugated Dendrimers Are a Tunable, High Performance CEST MRI NanoPlatform. Nano Letters, 2016, 16, 2248-2253.	9.1	43
54	Two decades of dendrimers as versatile <scp>MRI</scp> agents: a tale with and without metals. Wiley Interdisciplinary Reviews: Nanomedicine and Nanobiotechnology, 2018, 10, e1496.	6.1	42

#	Article	IF	CITATIONS
55	Noninvasive imaging of infection after treatment with tumorâ€homing bacteria using Chemical Exchange Saturation Transfer (CEST) MRI. Magnetic Resonance in Medicine, 2013, 70, 1690-1698.	3.0	39
56	Noninvasive monitoring of chronic kidney disease using pH and perfusion imaging. Science Advances, 2019, 5, eaaw8357.	10.3	38
57	Diamagnetic chemical exchange saturation transfer ( <scp>diaCEST</scp> ) liposomes: physicochemical properties and imaging applications. Wiley Interdisciplinary Reviews: Nanomedicine and Nanobiotechnology, 2014, 6, 111-124.	6.1	36
58	Microencapsulated cell tracking. NMR in Biomedicine, 2013, 26, 850-859.	2.8	34
59	Feasibility of concurrent dual contrast enhancement using CEST contrast agents and superparamagnetic iron oxide particles. Magnetic Resonance in Medicine, 2009, 61, 970-974.	3.0	33
60	Non-invasive temperature mapping using temperature-responsive water saturation shift referencing (T-WASSR) MRI. NMR in Biomedicine, 2014, 27, 320-331.	2.8	33
61	Simultaneous water and lipid suppression for in vivo brain spectroscopy in humans. Magnetic Resonance in Medicine, 2005, 54, 691-696.	3.0	31
62	Anthranilic acid analogs as diamagnetic CEST MRI contrast agents that feature an intramolecularâ€bond shifted hydrogen. Contrast Media and Molecular Imaging, 2015, 10, 74-80.	0.8	28
63	Solid-State NMR and Density Functional Investigation of Carbon-13 Shielding Tensors in Metalâ^'Olefin Complexes. Journal of Physical Chemistry A, 1997, 101, 8908-8913.	2.5	27
64	Multiâ€echo Length and Offset VARied Saturation (MeLOVARS) method for improved CEST imaging. Magnetic Resonance in Medicine, 2015, 73, 488-496.	3.0	27
65	Detection and differentiation of Cys, Hcy and GSH mixtures by 19F NMR probe. Talanta, 2018, 184, 513-519.	5.5	27
66	Salicylic acid analogues as chemical exchange saturation transfer MRI contrast agents for the assessment of brain perfusion territory and blood–brain barrier opening after intra-arterial infusion. Journal of Cerebral Blood Flow and Metabolism, 2016, 36, 1186-1194.	4.3	24
67	CT and CEST MRI bimodal imaging of the intratumoral distribution of iodinated liposomes. Quantitative Imaging in Medicine and Surgery, 2019, 9, 1579-1591.	2.0	24
68	A Solid-State Nitrogen-15 Nuclear Magnetic Resonance Spectroscopic and Quantum Chemical Investigation of Nitrosoareneâ~Metal Interactions in Model Systems and in Heme Proteins. Journal of the American Chemical Society, 1998, 120, 1349-1356.	13.7	22
69	Measuring <i>in vivo</i> responses to endogenous and exogenous oxidative stress using a novel haem oxygenase 1 reporter mouse. Journal of Physiology, 2018, 596, 105-127.	2.9	22
70	Screening CEST contrast agents using ultrafast CEST imaging. Journal of Magnetic Resonance, 2016, 265, 224-229.	2.1	21
71	In vivo Magnetization Transfer MRI Shows Dysmyelination in an Ischemic Mouse Model of Periventricular Leukomalacia. Journal of Cerebral Blood Flow and Metabolism, 2011, 31, 2009-2018.	4.3	20
72	Biophysical Characterization of Human Protamine-1 as a Responsive CEST MR Contrast Agent. ACS Macro Letters, 2015, 4, 34-38.	4.8	19

#	Article	IF	CITATIONS
73	Diagnostic utility of tomographic myocardial perfusion imaging with technetium 99m furifosmin (Q12) compared with thallium 201: Results of a phase III multicenter trial1, 2. Journal of Nuclear Cardiology, 1996, 3, 291-300.	2.1	17
74	pH Imaging Using Chemical Exchange Saturation Transfer (CEST) MRI. Israel Journal of Chemistry, 2017, 57, 862-879.	2.3	17
75	Metabolites in ventricular cerebrospinal fluid detected by proton magnetic resonance spectroscopic imaging. Journal of Magnetic Resonance Imaging, 2004, 20, 496-500.	3.4	16
76	NOrmalized MAgnetization Ratio (NOMAR) filtering for creation of tissue selective contrast maps. Magnetic Resonance in Medicine, 2013, 69, 516-523.	3.0	16
77	Magnetization transfer contrast MRI for non-invasive assessment of innate and adaptive immune responses against alginate-encapsulated cells. Biomaterials, 2014, 35, 7811-7818.	11.4	16
78	<sup>15</sup> N Heteronuclear Chemical Exchange Saturation Transfer MRI. Journal of the American Chemical Society, 2016, 138, 11136-11139.	13.7	16
79	Chemical Exchange Saturation Transfer (CEST) Agents: Quantum Chemistry and MRI. Chemistry - A European Journal, 2016, 22, 264-271.	3.3	14
80	Freeâ€base porphyrins as CEST MRI contrast agents with highly upfield shifted labile protons. Magnetic Resonance in Medicine, 2019, 82, 577-585.	3.0	14
81	Developing MR Probes for Molecular Imaging. Advances in Cancer Research, 2014, 124, 297-327.	5.0	13
82	Photochemistry and Dynamics of Vinyl Bromide and Vinyl Iodide in Rare Gas Matrixes. The Journal of Physical Chemistry, 1995, 99, 10506-10510.	2.9	12
83	Potential detection of cancer with fluorinated silicon nanoparticles in <sup>19</sup> F MR and fluorescence imaging. Journal of Materials Chemistry B, 2018, 6, 4293-4300.	5.8	12
84	Redesigned reporter gene for improved proton exchange-based molecular MRI contrast. Scientific Reports, 2020, 10, 20664.	3.3	12
85	Time domain removal of irrelevant magnetization in chemical exchange saturation transfer Zâ€spectra. Magnetic Resonance in Medicine, 2013, 70, 547-555.	3.0	11
86	Cellular and Molecular Imaging Using Chemical Exchange Saturation Transfer. Topics in Magnetic Resonance Imaging, 2016, 25, 197-204.	1.2	11
87	Salicylic Acidâ€Based Polymeric Contrast Agents for Molecular Magnetic Resonance Imaging of Prostate Cancer. Chemistry - A European Journal, 2018, 24, 7235-7242.	3.3	11
88	Photochemistry of Hydrogen Bromide-Acetylene Complexes in Solid Krypton. The Journal of Physical Chemistry, 1994, 98, 11909-11917.	2.9	10
89	Steady pulsed imaging and labeling scheme for noninvasive perfusion imaging. Magnetic Resonance in Medicine, 2016, 75, 238-248.	3.0	10
90	A snapshot of the vast array of diamagnetic CEST MRI contrast agents. NMR in Biomedicine, 2023, 36, e4715.	2.8	10

#	Article	IF	CITATIONS
91	Determination of order parameters and correlation times in proteins: a comparison between Bayesian, Monte Carlo and simple graphical methods. Journal of Biomolecular NMR, 1999, 13, 133-137.	2.8	8
92	Dynamic Contrast Enhanced-MR CEST Urography: An Emerging Tool in the Diagnosis and Management of Upper Urinary Tract Obstruction. Tomography, 2021, 7, 80-94.	1.8	8
93	Protein and peptide engineering for chemical exchange saturation transfer imaging in the age of synthetic biology. NMR in Biomedicine, 2023, 36, e4712.	2.8	8
94	The evolution of MRI probes: from the initial development to stateâ€ofâ€ŧheâ€art applications. NMR in Biomedicine, 2013, 26, 725-727.	2.8	7
95	Amplified detection of phosphocreatine and creatine after supplementation using CEST MRI at high and ultrahigh magnetic fields. Journal of Magnetic Resonance, 2020, 313, 106703.	2.1	7
96	Molecular Imaging of CXCL12 Promoter-driven HSV1-TK Reporter Gene Expression. Biotechnology and Bioprocess Engineering, 2018, 23, 208-217.	2.6	6
97	Efficient temperature-feedback liposome for <sup>19</sup> F MRI signal enhancement. Chemical Communications, 2020, 56, 14427-14430.	4.1	6
98	Quantitative cerebrovascular reactivity <scp>MRI</scp> in mice using acetazolamide challenge. Magnetic Resonance in Medicine, 2022, 88, 2233-2241.	3.0	5
99	NMR and Quantum Chemistry of Proteins and Model Systems. ACS Symposium Series, 1999, , 40-62.	0.5	4
100	Analysis Protocol for the Quantification of Renal pH Using Chemical Exchange Saturation Transfer (CEST) MRI. Methods in Molecular Biology, 2021, 2216, 667-688.	0.9	4
101	Renal pH Imaging Using Chemical Exchange Saturation Transfer (CEST) MRI: Basic Concept. Methods in Molecular Biology, 2021, 2216, 241-256.	0.9	3
102	Screening of CEST MR Contrast Agents. Methods in Molecular Biology, 2011, 771, 171-187.	0.9	3
103	Renal pH Mapping Using Chemical Exchange Saturation Transfer (CEST) MRI: Experimental Protocol. Methods in Molecular Biology, 2021, 2216, 455-471.	0.9	2
104	Physical Mechanism and Applications of CEST Contrast Agents. , 2007, , 85-100.		2
105	Unlabeled aspirin as an activatable theranostic MRI agent for breast cancer. Theranostics, 2022, 12, 1937-1951.	10.0	2
106	Cancer Therapy: Vaginal Delivery of Paclitaxel via Nanoparticles with Nonâ€Mucoadhesive Surfaces Suppresses Cervical Tumor Growth (Adv. Healthcare Mater. 7/2014). Advanced Healthcare Materials, 2014, 3, 1120-1120.	7.6	0
107	Chapter 6 General Theory of CEST Image Acquisition and Post-Processing. , 2017, , 55-96.		0

108 Chapter 9 Current Landscape of diaCEST Imaging Agents. , 2017, , 159-192.

0